Neural Adhesion Molecule Close Homolog of L1 Deficiency Exacerbates DSS-Induced Colitis in Mice

Ying Han
Academy of Military Medical Sciences
Ling-Ling Zhu (linglingzhuamms@126.com)
Academy of Military Medical Sciences https://orcid.org/0000-0002-4929-7103
Xiaomeng Wang
Academy of Military Medical Sciences
Cheng Xiang
Academy of Military Medical Sciences
Ming Zhao
Academy of Military Medical Sciences
Tong Zhao
Academy of Military Medical Sciences
Liang Guo
Academy of Military Medical Sciences
Dan Liu
Academy of Military Medical Sciences
Kuiwu Wu
Academy of Military Medical Sciences
Ming Fan
Academy of Military Medical Sciences
Ming Shi
Academy of Military Medical Sciences

Research article

Keywords: CHL1, Dextran Sodium Sulfate (DSS), colitis, neutrophil, macrophage

Posted Date: April 13th, 2020

DOI: https://doi.org/10.21203/rs.3.rs-21945/v1

Abstract

Background: The cell adhesion molecule CHL1, which belongs to the immunoglobulin superfamily, functions in a variety of physiological and pathological processes including neural development, tissue injury and repair. Recently, we found CHL1 was co-localized with GFAP positive cells in mouse colon tissue.

Methods: Here, Colon tissues were collected from CHL1+/+ , CHL1+/- and CHL1-/- mice after dextran sodium sulfate (DSS) induced to investigate the effects of CHL1 on the development of DSS-induced colitis.

Results: The data showed that CHL1 expression was increased in distal colon in a time-dependent manner after DSS-treatment. CHL1 deficiency induced more pronounced colitis features, an exacerbation of inflammation and damage to colonic tissues in DSS-induced mouse than that of wild type mouse. Moreover, CHL1-/- mice showed a remarkable increase of neutrophil and macrophage infiltration into colonic tissues, and then result in more severe damage to the intestinal epithelial cells and FITC leakage in CHL1 deficiency mice than that in WT mouse.

Conclusions: Our results revealed a distinct colonic role for CHL1 in regulating DSS-induced colitis, CHL1 deficiency exacerbates DSS-induced colitis in mice, indicating that CHL1 may be an attractive therapeutic target for IBD.

Introduction

IBD, which encompass ulcerative colitis (UC) and Crohn's disease (CD),are chronic, idiopathic, relapsing disorders of the gastrointestinal tract (Xavier and Podolsky 2007). UC is characterized by inflammation that is limited to the colon. In UC, the pattern of inflammation of colonic mucosa includes the impairment of the immune response, breakdown of epithelial barrier, and the enhancement of inflammatory process. By contrast, CD involves any part of the gastrointestinal tract. The microscopic features of CD include thickened submucosa, transmural inflammation, fissuring ulceration, and non-caseating granulomas (Liu and Stappenbeck 2016).

Though the mechanisms of IBD remain unclear, it is viewed as the outcome of a multifactorial process involving alterations in innate immunity and immune response to bacteria, genetic predisposition and some environmental factors (Gaya et al. 2006). Genome-wide association studies have identified more variants associated with IBD. There are now more than 200 IBD risk loci. It is suggested that IBD is related to disorders of innate immune response, adaptive immunity, endoplasmic reticulum stress, autophagy, intestinal epithelial barrier function and microbial defense pathways (Liu et al. 2015). In patients with CD, the genes encoding adhesion molecules may lead to uncontrolled inflammation with ensuing destruction of epithelial cells, inappropriate stimulation of antimicrobial and T cells differentiation, and inflammasome events (Palmieri et al. 2015).

Adhesion molecules have been reported to regulate the recirculation of leukocytes. Leukocyte recruitment is pivotal for the initiation and perpetuation of IBD and controlled by the specificity and interactions of chemokines and adhesion molecules (Springer 1994). Interactions of the adhesion molecules a4b7-integrin and mucosal addressin cell-adhesion molecule-1 (MAdCAM-1) promote the accumulation of pathogenic T-cell populations in the inflamed intestine (Schippers et al. 2016). In addition, adhesion molecules maintain the intestinal barrier function that is crucial to prevent intestinal inflammation. Dual immunoglobulin domain-containing adhesion molecule (DICAM) has been recently identified and known for the involvement in cell-cell adhesion through homophilic interaction and heterophilic interaction with integrin αVβ3, which affects the severity of colonic inflammation (Jung et al. 2008).

The cell adhesion molecule CHL1, also known as L1CAM2, is a member of the immunoglobulin superfamily (IgSF). Previous reports have demonstrated CHL1 mainly participates in multiple aspects of neural development and regeneration after injury (Yamanaka et al. 2011; Zhang et al. 2000). Recent studies show that CHL1 is expressed not only in neurons, but also in astrocytes and leukocytes in circulation, which suggests that CHL1 has a variety of other important functions. The cell adhesion molecule L1 is highly homologous to CHL1 and blocking L1 inhibits T cell adhesion and attack to neurons in vitro. Down-regulation of neuronal L1, implicating the transcription repressor REST, is an adaptive attempt to promote neuronal self-defense in response to neuroinflammation (Menzel et al. 2016). Furthermore, It was reported that astrogliosis stimulated by bacterial lipopolysaccharide (LPS) upregulates CHL1 expression in primary cultures of mouse cerebral astrocytes, coinciding with elevated protein synthesis and translocation of protein kinaseδ (PKCδ) from cytosol to the membrane fraction (Wu et al. 2010). Our previous results have shown the colocalization of CHL1 with glial fibrillary acidic protein (GFAP) positive glial cells in mouse colon tissue (SFig1A). Here, we investigated the effects of CHL1 in the development of DSS-induced colitis.

To study the correlation between CHL1 and colitis, we employed $CHL1^{+/+}$, $CHL1^{+/-}$ and $CHL1^{-/-}$ mice in DSS-induced colitis model. We found that the level of CHL1 protein expression was increased in colon tissue of DSS induced mouse. CHL1 deficiency induced more pronounced colitis features, an exacerbation of inflammation and damage to colonic tissues in DSS-induced colitis than that of wild type mouse, $CHL1^{-/-}$ mice showed a remarkable increase of neutrophil and macrophage infiltration into colonic tissues. This study provides a novel functional role of CHL1 in regulating colitis.

Methods

Mice Models

In all experiments, the ethics guidelines for investigations in conscious animals were followed and experiments were approved by the Animal Care and Use Committee of Institute of Basic Medical Sciences. Wild-type ($CHL1^{+/+}$) mice were purchased from Laboratory Animal Center of the Academy of Military Medical Sciences. Mice ($CHL1^{-/-}$) that lacked CHL1 was described previously (Montag-Sallaz et al. 2002). The background of $CHL1^{-/-}$ mice is the C57BL/6 strain. The heterozygous mice ($CHL1^{+/-}$) was

propagated by breeding $CHL1^{-/-}$ mice with C57BL/6 mice; the offspring were genotyped at weaning age using an PCR assay. Male mice aged seven to eight-week-old were used in this study.

To explore the alternation of CHL1 level in response to colitis, $CHL1^{+/+}$ mice were fed with ad libitum access to drinking sterile water containing 2.2% dextran sulfate sodium (DSS, MP Biomedicals, US) for 7 days followed by normal drinking water for 2 days. Mice were euthanized on the 5^{th}, 7^{th}, 9^{th} days after the initiation of DSS treatment, respectively. Then the colon was removed and washed with PBS for the following assays.

To explore the effects of deficiency of CHL1 on the development of DSS-induced colitis, $CHL1^{+/+}$, $CHL1^{+/-}$ and $CHL1^{-/-}$ mice were exposed to ad libitum access to sterile water containing 1.5% DSS, given that the $CHL1^{-/-}$ mice and $CHL1^{+/-}$ mice were more sensitive to the DSS-induced colitis than $CHL1^{+/+}$ mice. The mice were euthanized on 9^{th} days after DSS exposure, and then the colon was removed for the following assays.

Immunofluorescence Staining

The mice were anesthetized with 1% sodium pentobarbital through intraperitoneal injection and perfused with chilled 0.9% saline to wash out circulating blood, followed by 4% paraformaldehyde. Colon tissues were collected from $CHL1^{+/+}$ mice and $CHL1^{-/-}$ mice, after each colon was dehydrated and frozen-sectioned at 9μm, the sections were blocked with 5% BSA for 30min at 37℃ and then incubated with specific primary antibody (CHL1, 1:50, R&D Technology, US) overnight at 4℃ before incubation with secondary antibody (Alexa Fluor 488, 1:500, Thermo, Waltham, MA) for 90min at 37℃. Nuclei were counterstained with DAPI-containing mounting medium (ZSGB-BIO, CN). Images were captured using a scanning confocal microscope (Nikon, Tokyo, Japan).

Western Blot

The lysates were prepared from mouse distal colon tissues and total protein content was quantified. Each sample was loaded onto an SDS-PAGE gel and separated by electrophoresis. Then the proteins were transferred to nitrocellulose membranes. After blocking, the specific primary antibodies (CHL1, 1:1000 dilution, R&D Technology; β-actin, 1:10000 dilution, Sigma) were applied overnight at 4℃. After washing, the membranes were incubated with HRP-conjugated rabbit-anti-goat (1:5000 dilution; Bio-Rad, Hercules, CA) or goat-anti-mouse secondary antibody (1:10000 dilution; Bio-Rad) for 1h at room temperature. The specific bands were revealed using an ECL detection kit (Bio-Rad).

Quantitative Real-Time PCR

Total RNA was extracted from distal intestinal tissue homogenates using TRIzol reagent (Invitrogen, Carlsbad, CA). cDNA was synthesized by reverse transcription kit (Vazyme Biotech Co.,Ltd, China) following the manufacturer's instructions. Real-time PCR was performed with SYBR Green master mix (Genstar Biotech, China) using a real-time PCR detection system as recommended by the manufacturer.

The following oligonucleotide primers were used: β-actin: forward: 5′-ACTGTCGAGTCGCGTCCA-3, reverse: 5′-GTCATCCATGGCGAACTGGT-3′; IL-1β: forward: 5′-TTCAGGCAGGCAGTATCACTC-3′, reverse: 5′-GAAGGTCCACGGGAAAGACAC-3′; IL-6: forward: 5′-AGTCCTTCCTACCCCAATTTCC-3′, reverse: 5′-TTGGTTAGCCACTCCTTC-3′; tumor necrosis factor (TNF)-α: forward: 5′-CCCTCACACTCAGATCATCTTCT-3′, reverse: 5′-GCTACGACGTGGGCTACAG-3′. Gene-specific expression was normalized to β-actin expression.

Assessment of Colitis Symptoms and Disease Activity Index

To explore the time-dependent effects of DSS treatment in CHL1$^{+/+}$ mice, animal body weight was evaluated daily. To explore the effects of deficiency of CHL1 on the development of DSS-induced colitis, the animal body weight, stool consistency and the presence of rectal gross blood were individually evaluated daily. Each parameter was assigned a score according to the criteria previously proposed (Bibi et al. 2017; da Silva et al. 2016) and used to calculate on average daily the Disease Activity Index (DAI) (Supplementary Table 1).

Histological Staining

The mice were perfused with saline to wash out circulating blood cells under anesthesia. Subsequently, the colon tissues were collected from mice and the length was measured in a relaxed position without stretching. Then the colon tissues were fixed in 10% buffered formaldehyde and embedded in paraffin. Colon tissue were cut and stained with H&E. H&E staining tissue sections were scanned by Nanozoomer-XR Scanner C12000 (Hamamatsu Inc, JP) or taken on an Olympus BX51 microscope (Olympus, JP) using the Spot insight image capture system CCD camera.

Histological Scoring

To explore the effects of deficiency of CHL1 on the development of DSS-induced colitis by histological scoring, over 100 fields were photographed for each group. Each field was evaluated for tissue damage and inflammatory cell infiltration by two independent pathologists in a blinded manner. Tissue damage was assessed as follows: 1 (normal), no mucosal damage; 2 (mild), punctuate mucosal erosions; 3 (moderate), focal ulceration or surface mucosal erosion; 4 (severe), extensive mucosal damage and extension into deeper structures of the bowel wall. Inflammatory cell infiltration was assessed as follows: 1 (normal), occasional presence of inflammatory cells in the lamina propria; 2 (mild), increased presence of inflammatory cells in the lamina propria; 3 (moderate), confluence of inflammatory cells infiltrating into the submucosa; 4 (severe), transmural extension of the inflammatory cells. The data represent the percentage of fields for Normal, Mild, Moderate, and Severe in all fields for each group.

Intestinal Permeability Assay in Vivo

The intestinal permeability was measured by determining the amount of FITC-dextran in blood after it was orally administered as described previously (Xie et al. 2014). At the 5th day, mice were gavaged with

0.6mg/g body weight of FITC-Dextran (Sigma-Aldrich, UK) for 4h, and the blood samples were taken from hepatic vein. The blood sample were firstly centrifuged (3,000rpm, 4℃, 30min), and serum was collected and added to a 96-well microplate. The concentration of FITC was tested by Fluoroskan Ascent Fc (Thermo Scientific, US) with excitation wave 480 nm and emanation wave 530nm using serially diluted samples of the marker as standard. Then the colon tissues were cleaned with ice-cold PBS. The distribution of FITC-dextran in sectioned colonic tissue was determined by Nikon Ti-A1 fluorescent inverted microscope (Nikon Corporation, JP).

Immunohistochemical Staining

Immunohistochemical staining was performed as previously described (Carrascal et al. 2018). The sections were dewaxed in xylene and gradually hydrated in a decreasing ethanol series ending in distilled water. Endogenous peroxidase activity was quenched using 3% hydrogen peroxide in distilled water and then washed in PBS. After antigen retrieval by boiling the slides in 1 mM EDTA buffer (pH 8.0) for 10min, the sections were blocked with 5% BSA in PBS for 40min at 37℃. Then, the sections were incubated with the anti-Ly6B.2 (1:200 dilution, AbD Serotec, UK) or anti-F4/80 (1:1000 dilution, Servicebio, CN) antibody in PBS containing 5% BSA overnight at 4℃. For CHL1 staining, the sections, in which the antigen retrieval was performed by boiling the slide in sodium citrate (pH 6.0), were incubated with the anti-CHL1 (1:1000 dilution; R&D Technology, US) antibody in PBS containing 5% BSA overnight at 4°C. Following washing with PBS, the sections were incubated with horseradish peroxidase-conjugated secondary antibodies (ZSGB-BIO, CN). The color was developed by incubation with 3, 3’-diaminobenzidine solution. The sections were then counterstained with hematoxylin, dehydrated, and mounted. Images were taken on an Olympus BX51 microscope (Olympus, JP) using the spot insight image capture system CCD camera. Staining was assessed microscopically by two independent pathologists in a blinded manner.

Statistical Analysis

All data presented are expressed as arithmetic mean ± SEM. All statistical analyses were performed using GraphPad Prism version 7.0. Null hypotheses were rejected at $p \geq 0.05$. For statistical comparisons between two groups, we first performed a Shapiro-Wilk normality test (Prism) to determine whether the data was likely normally distributed. For normally-distributed data, we used unpaired Student’s t tests to evaluate statistical significance of differences between the two groups. Statistically significant differences between groups were determined using one-way ANOVA followed by Dunnett’s test. two-way ANOVA followed by Bonferroni’s *post hoc* test for multiple comparisons. For all analyses, $P<0.05$ was considered statistically significant.

Results

The level of CHL1 Expression was Increased in DSS-induced Inflammatory Colitis

DSS-induced colitis mouse model is used in the present study (Ruiz et al. 2016). To validate the DSS-induced acute colitis model, wild type mice were exposed to ad libitum access to drinking sterile water

containing 2.2% DSS for 7 days, followed by normal drinking water for 2 days (Fig 1A). DSS-treated mice present colitis symptoms, as evidenced by a significant shorten of the colon (Fig 1C and 1D) and weight loss (Fig 1B). H&E staining showed apparent inflammation in DSS-treated groups, including extensive ulceration of the epithelial layer, edema, crypt damage of bowel wall, and leukocyte infiltration into the mucosa (Fig 1E).

The expression pattern and localization of CHL1 in colon tissue were not reported previously. In this study, immunofluorescence assays were employed to detect CHL1 expression in colon tissue of mice. Positive CHL1 staining orderly and distinctively formed large bundles in the muscle layers of the colon tissue in $CHL1^{+/+}$ mice. Positive CHL1 staining also exhibited small bundles, which sporadically localized in the submucosa. Meanwhile, positive CHL1 staining surrounded the large intestinal gland in a reticular manner (Fig 1F). We then detected the expression level of CHL1 protein in colon tissue in response to DSS-induced colitis by western-blot assay. DSS treatment evidently up-regulated CHL1 expression levels in mice colon tissue at 9^{th} day (Fig 1G and 1H). These data implied that CHL1 is related to the occurrence of colitis.

CHL1 Deficiency Augmented DSS-induced Colitis in Mice

To further assess the impact of CHL1 on the development of DSS-induced colitis, wild-type ($CHL1^{+/+}$), CHL1 heterozygous ($CHL1^{+/-}$) and CHL1 deficient ($CHL1^{-/-}$) mice were given access to 1.5% DSS-containing drinking water ad libitum (Fig 2A). At baseline and throughout the course of treatment, we tracked these features on daily basis. DSS-induced injury reproduces some clinical features of human colitis including weight loss, diarrhea, and bloody stools. All control ($CHL1^{+/+}$, $CHL1^{+/-}$ and $CHL1^{-/-}$) mice were negative for weight loss, diarrhea and fecal blood. As expected, the body weights in $CHL1^{+/+}$, $CHL1^{+/-}$ and $CHL1^{-/-}$ mice were decreased after DSS treatment. The weight of $CHL1^{+/+}$ was significantly higher than that of $CHL1^{+/-}$ and $CHL1^{-/-}$ mice at 8^{th}, 9^{th} days after DSS-treatment (Fig 2B). The DAI (Disease activity index, DAI) score of $CHL1^{-/-}$ and $CHL1^{+/-}$ mice were significantly higher than that of $CHL1^{+/+}$ mice on day 7, day 8 and day 9 after DSS induced mouse (Fig 2C). These findings demonstrated that deficiency of CHL1 exacerbated DSS-induced colitis and implied a critical role of CHL1 in IBD.

Moreover, we observed that the length of colon tissue in DSS-induced $CHL1^{-/-}$ mice were significantly shorter than $CHL1^{+/+}$ mice (Fig 2D and 2E). Importantly, H&E staining presented more severe colitis symptom in DSS-induced $CHL1^{+/-}$ mice compared with DSS-induced $CHL1^{+/+}$ mice. Meanwhile, the colon tissue of $CHL1^{-/-}$ mice, compared with $CHL1^{+/-}$ and $CHL1^{+/+}$ mice, exhibited severe inflammation and crypt damage (Fig 2F). The pathological changes of colonic tissue, including inflammatory cell infiltration and tissue damage were scored. The histology scores in the mice of DSS groups were increased. DSS-induced $CHL1^{+/-}$ mice had a significantly higher inflammatory score and tissue damage than DSS-treated $CHL1^{+/+}$ group. Moreover, the colon tissue of $CHL1^{-/-}$ group had a significantly higher inflammatory score and damage than $CHL1^{+/-}$ and $CHL1^{+/+}$ group after DSS-treatment (Fig2G and 2H). However, all control mice ($CHL1^{+/+}$, $CHL1^{+/-}$ and $CHL1^{-/-}$) were negative for inflammatory cell infiltration

and tissue damage in colon tissue. The inflammatory cytokines IL-1β, IL-6, and TNF-α in the distal colon tissue were then measured by using real-time PCR, The data showed that the level of IL-6 in $CHL1^{-/-}$ mice after DSS treatment was increased significantly, while the levels of IL-1β and TNF-a showed an increasing trend (Fig2I, 2L and 2M). These results fully proved that the deficiency of CHL1 exacerbated the development of DSS-induced colitis.

The Deficiency of CHL1 Aggravated Epithelial Barrier Function in Mice

The above results exhibited that $CHL1^{-/-}$ mice had more severe colitis and more significant phenotypes. The intestinal epithelial cell density plays a key role in epithelial barrier function (Yu et al. 2015). to further address the effects of CHL1 deficiency, the intestinal epithelial barrier, intestinal barrier function was measured in $CHL1^{+/+}$ and $CHL1^{-/-}$ mice after DSS treatment. We carried out high magnification microscopic analysis of mucosal structure in $CHL1^{+/+}$ and $CHL1^{-/-}$ mice after DSS induced. Decreased intestinal epithelial cell density was observed after DSS treatment. Compared to $CHL1^{+/+}$ mice, $CHL1^{-/-}$ mice, displayed lower epithelial density in colonic tissues, more disorganized columnar epithelial cells and augmented cell volume (Fig 3A). In order to assay the intestinal barrier function, mice were given an oral dose of FITC-dextran on the 5^{th} day after DSS exposure, and FITC level in the serum was determined 4 hours later as a measure of intestinal permeability. DSS exposure induced a gentle increase in intestinal permeability as reflected by increased appearance of FITC in the serum in $CHL1^{+/+}$ while it was markedly increased in $CHL1^{-/-}$ mice (Fig 3B). The distribution of FITC-dextran in sectioned colonic tissue was evaluated by fluorescence microscopy. The results showed retention of FITC at the barrier in $CHL1^{+/+}$ mice. However, FITC had transcended the epithelial barrier after DSS exposure in $CHL1^{-/-}$ mice. The assay of relative intensity of FITC suggested that CHL1 deficiency impaired the intestinal barrier function in colitis (Fig 3C). These data suggested that the detrimental effects of CHL1 deficiency could be due to decreased epithelial barrier function as a result of disordered intestinal epithelial cell arrangement and density.

The Deficiency of CHL1 Induced Inflammatory Cell Infiltration

Neutrophils are key inflammatory cells in innate defense against invading pathogens. The egress and recruitment of neutrophils to the site of inflammation are tightly controlled in physiological and pathological conditions. Excessive neutrophil infiltration contributes to tissue damage in inflammatory disorders (Kolaczkowska and Kubes 2013). It has been proposed that neutrophil recruitment/infiltration is directly related to increased pathological damage in the experimental colitis, although their relative contributions to the pathogenesis of IBD are still controversial (Davies and Abreu 2015). The immunohistochemical staining with antibody against Ly6B as a marker of neutrophil showed that the neutrophils infiltration in colon tissue of $CHL1^{-/-}$ mice was significantly higher than $CHL1^{+/+}$ mice after DSS treatment (Fig 4A and 4B), which suggested that CHL1 was probably related to the changes of neutrophils infiltration.

Macrophage is an important element of the innate immune system, exhibiting a high heterogeneity of two subtypes. The number of macrophages was always increased by the inflammation enhanced in IBD (Kmieć et al. 2017). In order to explore the effect of the lack of CHL1 on macrophages infiltration in DSS-induced mice, colon tissue is observed by immunohistochemical staining with the antibody against F4/80 as a marker of macrophage. The macrophages infiltration of $CHL1^{-/-}$ mice was significantly higher than $CHL1^{+/+}$ mice in DSS-induced colitis (Fig 4C and 4D). The data suggested that the changes of neutrophils and macrophages infiltration were likely involved to CHL1 deficiency.

Discussion

Here, we provide new information regarding the impact of CHL1 on DSS-induced colitis. The data showed that CHL1 expression was increased in distal colon in a time-dependent manner in DSS-induced colitis. Deficiency of CHL1 exacerbated the development of DSS-induced colitis with pronounced colitis features including increasing in the pro-inflammatory cytokines, the leakage of FITC in colon and serum. These results suggested that CHL1 could be involved in regulating the occurrence and development of IBD.

The intestinal epithelium can be easily disrupted during gut inflammation as seen in IBD (Gitter et al. 2001). The intestinal epithelium might play a major role in the development and perpetuation of IBD (Wyatt et al. 1993). In the present study, during the initiation of DSS, intestinal epithelium functions are impaired and substantially precede the development of colitis in CHL1 deficiency mice. Meanwhile, the distribution of FITC-dextran in sectioned colonic tissue was evaluated after DSS introduced $CHL1^{-/-}$ mice. However, we found that CHL1 expression is not in intestinal epitheliums (data not shown). Interestingly, CHL1 is predominantly expressed in enteric glial (SFig1). Enteric glia are distributed throughout the laminar structure of the gastrointestinal tract and closely appose neurons, immune cells, blood vessels and the intestinal epithelium (Fu et al. 2013). Mucosal glia in the lamina propria directly underlie the epithelium, and this closed proximity raised the possibility that enteric glia plays a role in regulating epithelial functions such as cellular proliferation and barrier maintenance. When the GFAP promoter is used to express cellular toxins that eliminate glia in mice, intestinal epithelial permeability and proliferation increase, leading to translocation of luminal bacteria and intestinal inflammation (Bush et al. 2001). Therefore, consistent with this, CHL1 deficiency in enteric glial showed damage to colonic tissues and increasing the leakage of FITC in colon and serum. And then resulted in the development of DSS-induced colitis.

In addition, adhesion molecules have been reported to maintain the intestinal barrier function that is crucial to prevent intestinal inflammation (Han et al. 2019). Inflammatory cytokine expression is associated with the severity of IBD. Excessive pro-inflammatory cytokines can damage the colon mucosa and affect intestinal homeostasis. Pro-inflammatory cytokines, including IL-1β, IL-6 and TNF-α, have been implicated in the pathophysiology of IBD (Chi et al. 2018; Neurath 2014). We tested whether the change of CHL1 expression affected the colonic inflammation. We did find that CHL1 expression was increased in a time-dependent manner during development of DSS-induced colitis. Coincide with this, CHL1 expression increased in response to LPS-induced brain astrocyte activation by NF-κB signaling (Wu et al.

2010). However, contradicting with this, in this study,IL-6 expression is significantly increased in the colonic tissue in CHL1$^{-/-}$ group after DSS administration, as well as the number of neutrophils and macrophages. That may be related to different regulatory mechanisms of gut and brain tissue. Therefore, the precise mechanism of CHL1 deficiency in regulation of inflammation during colitis need to address future.

Recently, a new role for CHL1 outside the nervous system has emerged. It was found that CHL1 is a significant factor during the malignant progression of cancer. However, the functional roles of CHL1 in physiological and pathological process are poorly explored. Downregulation of CHL1 was detected in several types of tumor (such as stomach, rectum, colon, small intestine, pancreatic, kidney, bladder, breast, thyroid, vulva and skin cancer), suggesting that CHL1 might act as a putative tumor suppressor (Senchenko et al. 2011). Interestingly, CHL1 gene is hyper-methylated in DNA samples of African Americans patients with colorectal carcinoma. It has been known that patients with IBD are at increased risk for the development of colorectal cancer than general population (Lasry et al. 2016) and the same alleles overlapped in colorectal cancer and IBD in mouse model (Kraak 2015; Johnson et al. 2016; Ryan et al. 2014). IBD, which is mediated by chronic intestinal inflammation, is widely accepted as one of the main risk factors leading to colorectal cancer (Kim and Chang 2014). Whether CHL1 plays a potential role in colon cancer development through its regulation over the inflammatory processes of the intestine remains to be elucidated.

Conclusions

This work evidenced that the CHL1 deficiency aggravated the occurrence and development of DSS-induced colitis with pronounced colitis features, including destroy epithelial barrier function and enhanced the inflammation and damage to colonic tissues in DSS-induced colitis in mice. These results suggested that CHL1 could be involved in regulating the occurrence and development of colitis, which provides a novel functional role of CHL1 in regulating IBD.

Abbreviations

DSS: dextran sodium sulfate; IBD: Inflammatory bowel diseases; UC: ulcerative colitis; CD: Crohn's disease; MAdCAM-1: mucosal addressin cell-adhesion molecule-1; DICAM: Dual immunoglobulin domain-containing adhesion molecule; IgSF: immunoglobulin superfamily; LPS: lipopolysaccharide; PKCδ: protein kinaseδ; GFAP: glial fibrillary acidic protein; DAI: Disease Activity Index

Declarations

Ethics approval and consent to participate

Animals were handled in strict accordance with the Guidelines for the Institutional Animal Care and Use Committee of Institute of Cognition and Brain Sciences (NO. IACUC-2017049) and all studies complied

with the guidelines. During the study, tissue collection procedures were devised to minimize potential pain and distressed animals used.

Consent for publication

Not applicable

Availability of data and materials

All data generated or analyzed during this study are included in this published article and its supplementary information files.

Competing interests

The authors declare that they have no competing interests

Funding

This work is supported by National Natural Science Foundation of China (No. 81430044, 81773086, 81773258 and 81572845).

Authors' contributions

X.W. Y.H. M.S. and L.L. conceptualized the study; Y.H. and X.W. prepared and maintained $CHL1^{+/+}$、$CHL1^{+/-}$ and $CHL1^{-/-}$mice; Y.H. and X.W. designed and performed morphological analysis and biochemical assays; X.W. Y.H. wrote the manuscript. L.L., M.S. and L.G. discussed and edited the manuscript. M.Z., K.W. and X.C. supervised the project. All authors reviewed and gave final approval to the manuscript.

Acknowledgements

Not applicable

Author details

[1]Academy of Military Medical Sciences, Institute of Military Cognition and Brain Sciences, Beijing 100850, China. [2]Jiangsu Center for the Collaboration and Innovation of Cancer Biotherapy, Cancer Institute, Xuzhou Medical University, Xuzhou, 221000, China. [3]Co-Innovation Center of Neuroregeneration, Nantong University, Nantong, 226001, China. [4]Center for Brain Disorders Research, Capital Medical University, Beijing Institute of Brain Disorders, Beijing 100069, China.

References

Bibi, S., et al. Dietary Green Pea Protects against DSS-Induced Colitis in Mice Challenged with High-Fat Diet. Nutrients. 2017;9:

Bush, T. G., et al. Fulminant Jejuno-Ileitis following Ablation of Enteric Glia in Adult Transgenic Mice. 2001;120:A186-A187.

Carrascal, M. A., et al. Staining of E-selectin ligands on paraffin-embedded sections of tumor tissue. BMC Cancer. 2018;18:495.

Chi, J.-H., et al. Oregonin inhibits inflammation and protects against barrier disruption in intestinal epithelial cells. International immunopharmacology. 2018;59:134-140.

da Silva, L. M., et al. Hydroalcoholic Extract from Inflorescences of Achyrocline satureioides (Compositae) Ameliorates Dextran Sulphate Sodium-Induced Colitis in Mice by Attenuation in the Production of Inflammatory Cytokines and Oxidative Mediators. Evid Based Complement Alternat Med. 2016;2016:3475356.

Davies, J. M. & M. T. Abreu. The innate immune system and inflammatory bowel disease. Scand J Gastroenterol. 2015;50:24-33.

Fu, Y. Y., et al. 3-D imaging and illustration of mouse intestinal neurovascular complex. 2013;304:G1-G11.

Gaya, D. R., et al. New genes in inflammatory bowel disease: lessons for complex diseases? 2006;367:1271-1284.

Gitter, A. H., et al. Epithelial barrier defects in ulcerative colitis: characterization and quantification by electrophysiological imaging. Gastroenterology. 2001;121:1320-8.

Han, S. W., et al. DICAM Attenuates Experimental Colitis via Stabilizing Junctional Complex in Mucosal Barrier. Inflamm Bowel Dis. 2019;25:853-861.

Johnson, D. H., et al. DNA Methylation and Mutation of Small Colonic Neoplasms in Ulcerative Colitis and Crohn's Colitis: Implications for Surveillance. Inflamm Bowel Dis. 2016;22:1559-67.

Jung, Y. K., et al. DICAM, a novel dual immunoglobulin domain containing cell adhesion molecule interacts with αvβ3 integrin. Journal of Cellular Physiology. 2008;216:603-614.

Kim, E. R. & D. K. Chang. Colorectal cancer in inflammatory bowel disease: the risk, pathogenesis, prevention and diagnosis. World J Gastroenterol. 2014;20:9872-81.

Kmieć, Z., et al. Cells of the innate and adaptive immunity and their interactions in inflammatory bowel disease. Adv Med Sci. 2017;62:1-16.

Kolaczkowska, E. & P. Kubes. Neutrophil recruitment and function in health and inflammation. Nat Rev Immunol. 2013;13:159-75.

Kraak, L. V. D. Colitis-associated colon cancer: Is it in your genes? World Journal of Gastroenterology. 2015;21:11688.

Lasry, A., et al. Inflammatory networks underlying colorectal cancer. Nat Immunol. 2016;17:230-40.

Liu, J. Z., et al. Association analyses identify 38 susceptibility loci for inflammatory bowel disease and highlight shared genetic risk across populations. Nat Genet. 2015;47:979-986.

Liu, T. C. & T. S. Stappenbeck. Genetics and Pathogenesis of Inflammatory Bowel Disease. Annu Rev Pathol. 2016;11:127-48.

Menzel, L., et al. Down-regulation of neuronal L1 cell adhesion molecule expression alleviates inflammatory neuronal injury. Acta neuropathologica. 2016;132:703-720.

Montag-Sallaz, M., et al. Misguided axonal projections, neural cell adhesion molecule 180 mRNA upregulation, and altered behavior in mice deficient for the close homolog of L1. Mol Cell Biol. 2002;22:7967-81.

Neurath, M. F. Cytokines in inflammatory bowel disease. Nature reviews. Immunology. 2014;14:329-342.

Palmieri, O., et al. Genome-wide Pathway Analysis Using Gene Expression Data of Colonic Mucosa in Patients with Inflammatory Bowel Disease. Inflamm Bowel Dis. 2015;21:1260-8.

Ruiz, P. A., et al. Titanium dioxide nanoparticles exacerbate DSS-induced colitis: Role of the NLRP3 inflammasome. Gut. 2016;66:

Ryan, B. M., et al. An analysis of genetic factors related to risk of inflammatory bowel disease and colon cancer. Cancer Epidemiol. 2014;38:583-90.

Schippers, A., et al. β7-Integrin exacerbates experimental DSS-induced colitis in mice by directing inflammatory monocytes into the colon. Mucosal Immunol. 2016;9:527-38.

Senchenko, V. N., et al. Differential expression of CHL1 gene during development of major human cancers. PLoS One. 2011;6:e15612.

Springer, T. A. Traffic signals for lymphocyte recirculation and leukocyte emigration: the multistep paradigm. Cell. 1994;76:301-14.

Wu, J., et al. Phosphatidylinositol 3-kinase/protein kinase Cdelta activation induces close homolog of adhesion molecule L1 (CHL1) expression in cultured astrocytes. Glia. 2010;58:315-28.

Wyatt, J., et al. Intestinal permeability and the prediction of relapse in Crohn's disease. Lancet. 1993;341:1437-9.

Xavier, R. J. & D. K. Podolsky. Unravelling the pathogenesis of inflammatory bowel disease. Nature. 2007;448:427-34.

Xie, L., et al. Hypoxia-inducible factor/MAZ-dependent induction of caveolin-1 regulates colon permeability through suppression of occludin, leading to hypoxia-induced inflammation. Mol Cell Biol. 2014;34:3013-23.

Yamanaka, H., et al. Increase of close homolog of cell adhesion molecule L1 in primary afferent by nerve injury and the contribution to neuropathic pain. J Comp Neurol. 2011;519:1597-615.

Yu, S. J., et al. CARD3 deficiency protects against colitis through reduced epithelial cell apoptosis. Inflammatory bowel diseases. 2015;21:862-869.

Zhang, Y., et al. Expression of CHL1 and L1 by Neurons and Glia Following Sciatic Nerve and Dorsal Root Injury. Molecular & Cellular Neuroscience. 2000;16:71-86.

Figures

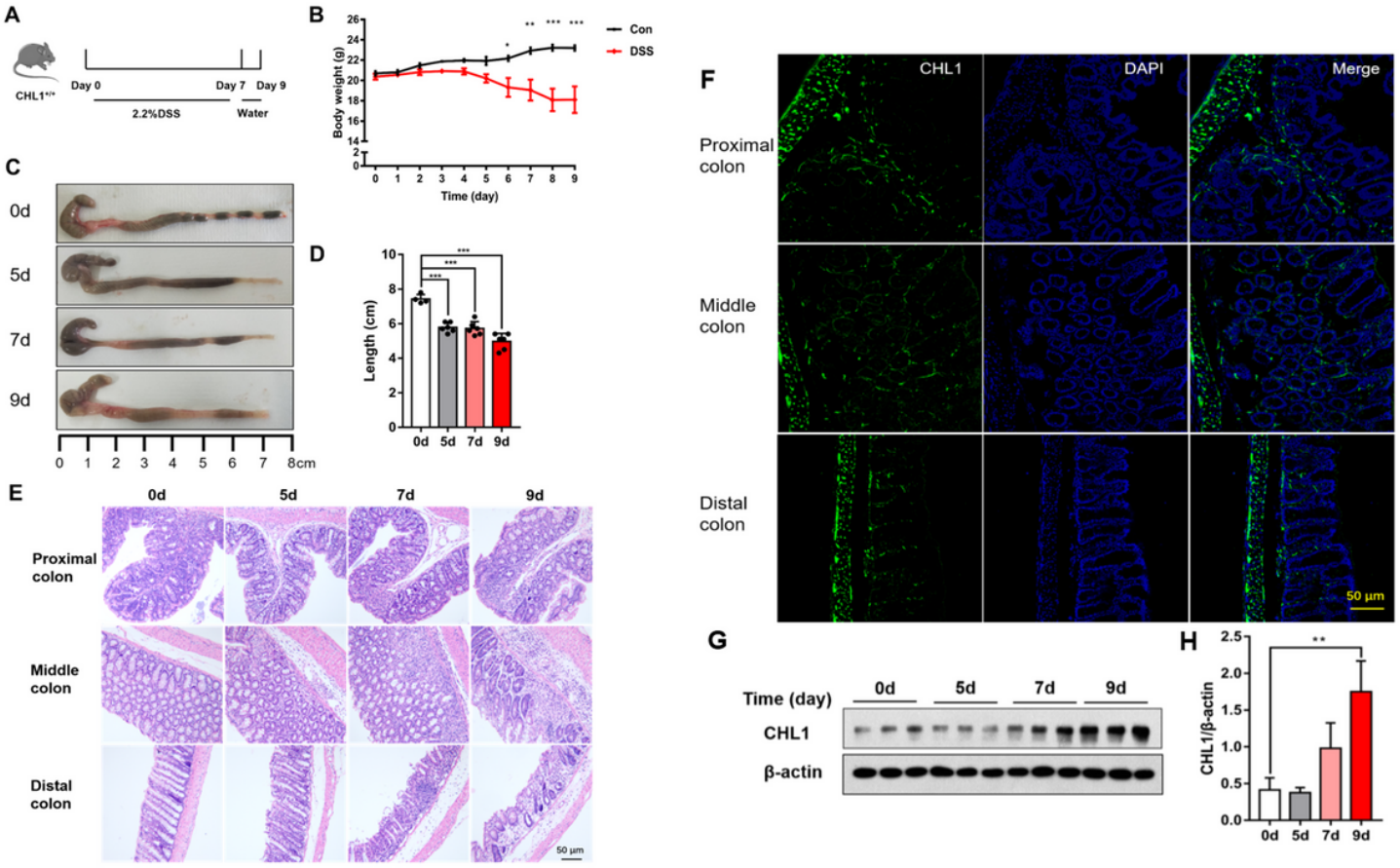

Figure 1

The Level of CHL1 Expression was Increased in DSS-induced Colitis (A) DSS-induced acute colitis mice model. CHL1+/+ mice were exposed to ad libitum access to drinking sterile water containing 2.2% DSS for 7 days followed by normal drinking water for 2 days. Mice were euthanized on the 5th, 7th, 9th day after the initiation of DSS treatment, respectively. (B) Body weight loss in DSS-induced acute colitis mice

model (*p < 0.05, **p < 0.01, ***p < 0.001, n = 4-6/group). (C, D) Colon section obtained from mice were analyzed for their outward appearance; Time-dependent effects of DSS treatment on colon length (***p < 0.001; n = 4-6/group). (E) Time-dependent effects of DSS treatment on representative histologic images of colonic tissue taken from CHL1+/+ mice. (F) CHL1(green) expression is detected in the colon tissue of mice by using immunofluorescence assay. (G, H) Western blots (G) and analysis (H) showing the time-dependent effects of DSS treatment on CHL1 expression in the colon tissue of CHL1+/+ mice (**p < 0.01, n = 3/group).

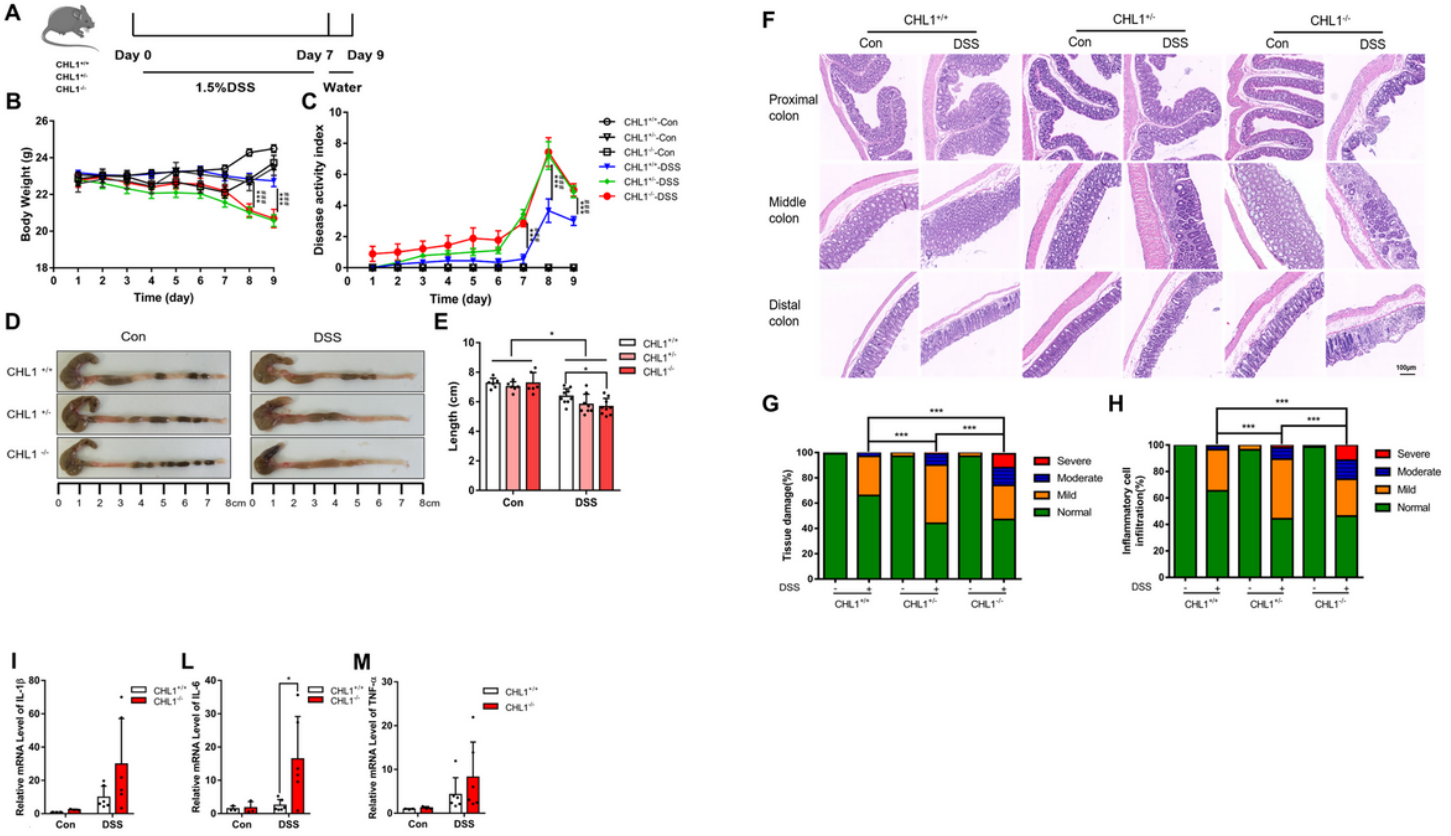

Figure 2

CHL1 Deficiency Augmented DSS-induced Colitis in Mice (A) DSS-induced acute colitis mice model. CHL1+/+, CHL1+/- and CHL1-/- mice were exposed to ad libitum access to drinking sterile water containing 1.5% DSS for 7 days followed by normal drinking water for 2 days. Mice were euthanized on the 9th day after the initiation of DSS treatment. (B, C) Body weight loss and the disease activity index score in CHL1+/+, CHL1+/- and CHL1-/- mice exposed to DSS. (DSS-induced CHL1+/+ group v.s DSS-induced CHL1+/- group, *** P < 0.001, n = 6-9/group; DSS-induced CHL1+/+ group v.s DSS-induced CHL1-/- group, ### P < 0.001, n = 6-9/group). (D, E) Colon section obtained from mice were analyzed for their outward appearance; Colon length in CHL1+/+, CHL1+/- and CHL1-/- mice exposed to DSS (*p < 0.05, n = 6-9/group). (F) Representative histologic images of colonic tissue taken from CHL1+/+, CHL1+/- and CHL1-/- mice with and without DSS treatment. (G, H) The histology score of tissue damage and inflammatory cell infiltration in CHL1+/+, CHL1+/- and CHL1-/- mice with and without DSS treatment (***p < 0.001, n = 6-9/group). (I, L, M) Real-time PCR analysis of changes of the inflammatory cytokines

IL-1β, IL-6, and TNF-a in the distal colon of mice, the increase of IL-6 expression in CHL1-/- mice after DSS treatment was significant (*p < 0.05, n = 4-6/group).

Figure 3

The Deficiency of CHL1 Aggravated Epithelial Barrier damage in IBD (A) High magnification histologic images of colonic tissue from CHL1+/+ and CHL1-/- mice with and without DSS treatment showed altered intestinal epithelial cellular shape in tissues from CHL1-/- animals. Insets show examples of areas of epithelium in ultra-high magnification. (B) Intestinal permeability was measured by the appearance of orally administered FITC-labeled dextran in serum from CHL1+/+ and CHL1-/- mice exposed to DSS (***p < 0.001, n = 5/group). (C) The relative grayscale of fluorescence microscopy of the intestinal mucosa from DSS-treated CHL1+/+ and CHL1-/- mice exposed to orally administered FITC-labeled dextran (***p < 0.001, n = 5/group).

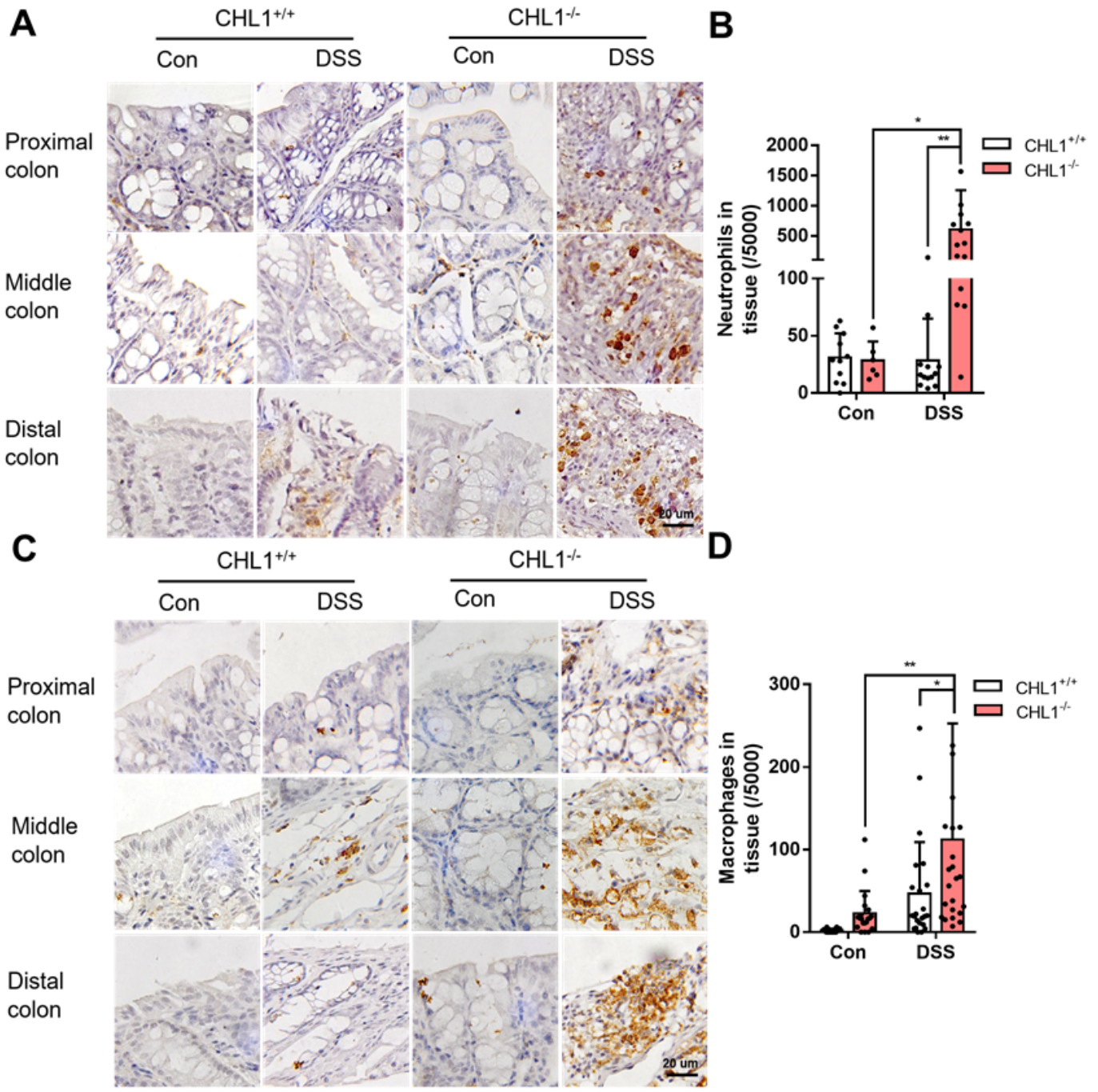

Figure 4

The Deficiency of CHL1 Induced Inflammatory Cell Infiltration (A, B) Representative immunohistochemical images (A) and analysis (B) of colon tissue measured by Ly6B.2 staining from CHL1+/+ and CHL1-/- mice exposed to DSS (*p<0.05, **p<0.01, n=5/group). (C, D) Representative immunohistochemical images (C) and analysis (D) in CHL1+/+ and CHL1-/- mice exposed to DSS as measured by F4/80 staining (*p < 0.05, **p < 0.01, n = 5/group).

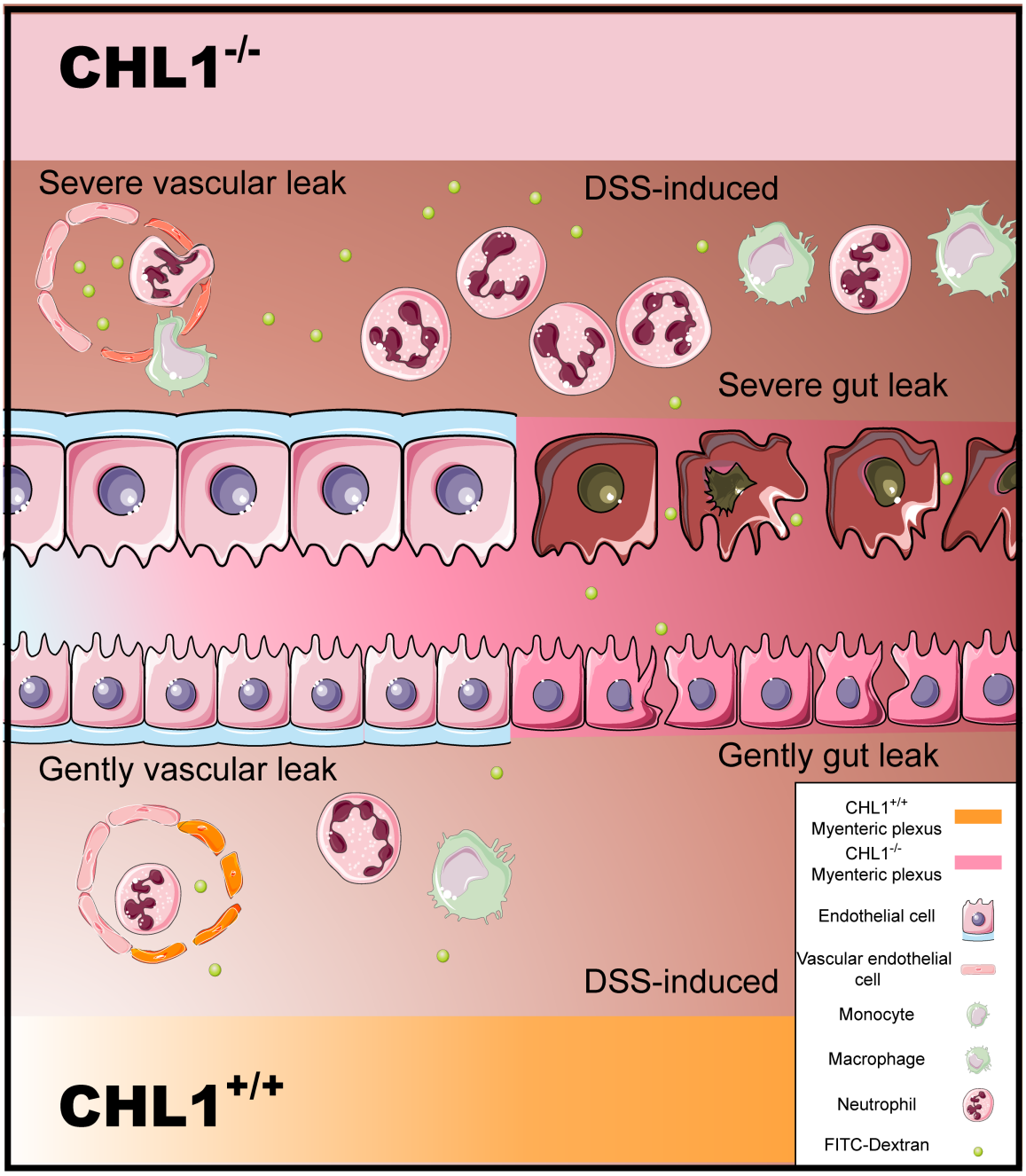

Figure 5

Model of CHL1 Deficiency Exacerbates Mice Colitis The loss of CHL1 exacerbates DSS-induced mice colitis. The deficiency of CHL1 aggravate epithelial barrier function and enhances the inflammation cell infiltrating epithelial in mice. Accordingly, we see more serious colitis in CHL1-/- mice after DSS induction.

Supplementary Files

This is a list of supplementary files associated with this preprint. Click to download.

- SupplementaryMaterialsBMC.docx
- SFig1.tif